# The Fe Protein Cycle Associated with Nitrogenase Catalysis Requires the Hydrolysis of Two ATP for Each Single Electron Transfer Event

Zhi-Yong Yang<sup>♠</sup>\*, Artavazd Badalyan<sup>♠</sup>, Brian M. Hoffman<sup>♣</sup>, Dennis R. Dean<sup>♥</sup>, Lance C. Seefeldt<sup>♠</sup>\*

ABSTRACT: A central feature of the current understanding of dinitrogen (N2) reduction by the enzyme nitrogenase is the proposed coupling of the hydrolysis of two ATP, forming two ADP and two Pi, to the transfer of one electron from the Fe protein component to the MoFe protein component, where substrates are reduced. A redox-active [4Fe-4S] cluster associated with the Fe protein is the agent of electron delivery and it is well known to have a capacity to cycle between a one-electron-reduced [4Fe-4S]<sup>1+</sup> state and an oxidized [4Fe-4S]2+ state. Recently, however, it has been shown that certain reducing agents can be used to further reduce the Fe protein [4Fe-4S] cluster to a super-reduced, all-ferrous [4Fe-4S]<sup>0</sup> state that can be either diamagnetic (S = 0) or paramagnetic (S= 4). It has been proposed that the super-reduced state might fundamentally alter the existing model for nitrogenase energy utilization by the transfer of two electrons per Fe protein cycle linked to hydrolysis of only two ATP molecules. Here, we measure the number of ATP consumed for each electron transfer under steady-state catalysis while the Fe protein cluster is in the [4Fe-4S]<sup>1+</sup> state and when it is in [4Fe-4S]<sup>0</sup> state. Both oxidation states of the Fe protein are found to operate by hydrolyzing two ATP for each single-electron transfer event. Thus, regardless of its initial redox state, the Fe protein transfers only one electron at a time to the MoFe protein in a process that requires the hydrolysis of two ATP.

#### **INTRODUCTION**

The biological reduction of dinitrogen (N<sub>2</sub>) to two ammonia (NH<sub>3</sub>) is catalyzed by the enzyme nitrogenase.<sup>1</sup> For the Mo-dependent nitrogenase, the reaction requires two component proteins designated the Fe protein and MoFe protein, as well as ATP hydrolysis, and low-potential electrons (**Figure 1**).<sup>2–7</sup> There are two other nitrogenase isozymes designated as the V-dependent and Fe-only nitrogenases.<sup>8–13</sup> All three nitrogenase forms show the same basic mechanism, <sup>14,15</sup> so the Mo-dependent version is typically considered to represent the mechanistic paradigm for biological nitrogen fixation. <sup>14,16–19</sup> The reduction of N<sub>2</sub>, as well as other non-physiological substrates, by nitrogenase requires the delivery of electrons from the Fe protein to the MoFe protein in a reaction coupled to hydrolysis of ATP to ADP and inorganic phosphate (Pi).<sup>6</sup> In the absence of any other substrate, nitrogenase reduces protons to yield

H<sub>2</sub>. <sup>14</sup>, <sup>16</sup>, <sup>17</sup> The redox-active species contained within the Fe protein is a [4Fe-4S] cluster bridged between two identical protein subunits, each of which contains a MgATP binding site. <sup>20</sup>

The canonical model for the stoichiometry of MgATP hydrolysis required to achieve each electron transfer event was developed in the laboratory of Burris several decades ago.<sup>2</sup> According to that model, catalysis is initiated when the Fe protein, having its [4Fe-4S] cluster in the reduced (FePred, [4Fe-4S]1+) oxidation state and two bound MgATP molecules, associates with the MoFe protein.<sup>3</sup> One electron is then transferred from the Fe protein [4Fe-4S]<sup>1+</sup> cluster to the MoFe protein followed by the hydrolysis of the two ATP molecules to two ADP and two Pi. The cycle is completed by dissociation of the Fe protein from the MoFe protein. As noted, this series of events, called the Fe protein cycle, 6,21-23 results in the transfer of one electron to the MoFe protein and the hydrolysis of two ATP. After dissociation of the two catalytic partners, a new cycle can be initiated by re-reduction of the oxidized Fe protein (FePox, [4Fe-4S]<sup>2+</sup>) by a small redox protein such as ferredoxin or flavodoxin or by an artificial redox mediator such as dithionite (DT), and with two ATP molecules replacing the two ADP molecules. 4,6,24,25 Fe protein cycles are repeated until sufficient electrons have accumulated within the MoFe protein to achieve substrate binding and reduction to product. 14,21,26,27 In the case of N<sub>2</sub> reduction, 8 Fe protein cycles yields two NH<sub>3</sub> and the obligate evolution of one H<sub>2</sub>. 14,16,17,21,28,29 Thus, the reduction of one equivalent of N<sub>2</sub> requires the hydrolysis of 16ATP, representing a large energy demand.<sup>23</sup> In the absence of other substrates, MoFe protein acts as a hydrogenase, 30,31 utilizing two Fe protein cycles for reduction of two protons to yield one H<sub>2</sub> with hydrolysis of 4 ATP (Figure  $1A).^{2,7,32}$ 

As described above, the Fe protein [4Fe-4S] cluster has been typically considered to act as a one-electron carrier, utilizing the FeP<sup>ox</sup>/FeP<sup>red</sup> ([4Fe-4S]<sup>2+/1+</sup>) redox couple.<sup>23,33</sup> It has been more recently demonstrated that the Fe protein [4Fe-4S]<sup>1+</sup> cluster can be further reduced to a super-reduced state (FeP<sup>sr</sup>, [4Fe-4S]<sup>0</sup>) having all the associated Fe atoms in the ferrous (Fe(II)) oxidation state.<sup>34,35</sup> Two different spin states of this super-reduced cluster

<sup>\*</sup>Department of Chemistry and Biochemistry, Utah State University, Logan UT 84322, USA.

<sup>\*</sup>Departments of Chemistry and Molecular Biosciences, Northwestern University, Evanston, IL 60208, USA.

<sup>\*</sup>Department of Biochemistry, Virginia Tech, Blacksburg VA 24061, USA.

have been observed, an EPR-silent (perpendicular mode), non-Kramers state previously assigned as an S=0 state by an Evans NMR method (denoted as S=0 here),

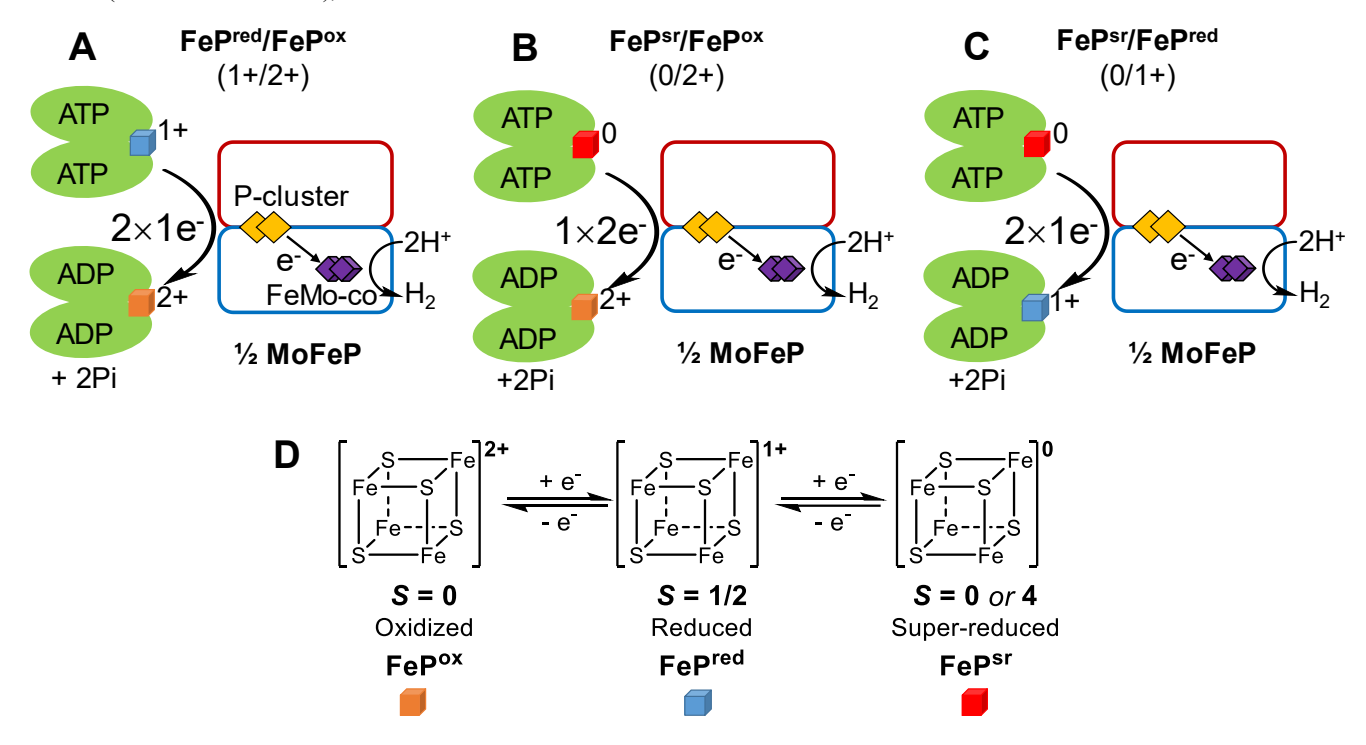


**Figure 1.** Nitrogenase Fe protein cycles. (A) One-electron reduced Fe protein (FePred) delivers one electron to one half of the MoFe protein (½ MoFeP) per Fe protein cycle with hydrolysis of two ATP to two ADP and two inorganic phosphate (Pi). Two such cycles are needed to reduce two protons to one H<sub>2</sub> molecule. (B) Two-electron reduced Fe protein (super-reduced, FePsr) might deliver two electrons to ½ MoFeP per cycle with hydrolysis of two ATP molecules. One such cycle would be needed to reduce two protons to one H<sub>2</sub> molecule. (C) FePsr might deliver one electron to ½ MoFeP per cycle with hydrolysis of two ATP molecules. Two cycles would be needed to produce one H<sub>2</sub> molecule. (D) Schematic representations of the Fe protein [4Fe-4S] cluster in three redox states with noted spin states (S).

 $^{34,36}$  and an S=4 state, whose EPR signal is observable with parallel-mode detection,  $^{35,37}$  with redox potentials for the FePred/FePsr couple of  $E_{\rm m}=$  -460 mV vs NHE for the S=0 state  $^{34,36}$  and  $E_{\rm m}=$  -790 mV for the S=4 state.  $^{38,39}$  The S=0 FePsr protein can be generated by treatment of the Fe protein with mild redox potential reductants such as one electron-reduced methyl viologen (MV\*+,  $E_{\rm m}=$  -450 mV)  $^{34}$  and a physiological reductant, the hydroquinone form of flavodoxin (FldHQ,  $E_{\rm m}\approx$  -460 to -520 mV).  $^{18,19,36}$  When the Fe protein is reduced with artificial reductants having very negative reduction potentials (e.g., Ti(III)-citrate, Cr(II)-EDTA, and Eu(II)-L,  $E_{\rm m}<$  -800 mV), the S=4 spin state of the FePsr is achieved.  $^{18,19,35,38,40,41}$ 

Discovery of FeP<sup>sr</sup> species raised the possibility that the Fe protein might cycle between the FeP<sup>sr</sup> and FeP<sup>ox</sup> states during each Fe protein cycle, thus simultaneously transferring two electrons coupled to the hydrolysis of two ATP (**Figure 1B**). <sup>18,19,34</sup> If such a couple were indeed operative, this would fundamentally change the existing concept of the energetics associated with nitrogenase catalysis, namely, to a requirement for the hydrolysis of only 8 ATP instead of 16 ATP for each N<sub>2</sub> reduction or hydrolysis of 2 ATP instead of 4 ATP for reduction of two protons to evolve one H<sub>2</sub>. <sup>18,19</sup>

Several reports have established that the two electrons carried by FePsr can be used to support nitrogenase catalysis. 34,42,43 However, the events associated with the transfer of electrons stored in FePsr have not been established. 36,42,44 Namely, are the two electrons transferred through one Fe protein cycle, with FePox/FePsr ([4Fe-4S]<sup>2+/0</sup>) as the operative redox couple and with hydrolysis of two ATP (1ATP per e transferred) (**Figure 1B**), 36,43 or through two consecutive Fe protein cycles with FePred/FePsr ([4Fe-4S]<sup>1+/0</sup>) and

FeP<sup>ox</sup>/FeP<sup>red</sup> ([4Fe-4S]<sup>2+/1+</sup>) as stepwise operative couples and hydrolysis of four ATP in total (2 ATP per e<sup>-</sup> transferred) (**Figure 1C**)? Earlier studies attempted to establish the nature of the coupling of electron transfer and ATP hydrolysis involving the superreduced Fe protein and concluded that it was possible that the FeP<sup>ox</sup>/FeP<sup>sr</sup> couple exhibited a stoichiometry of 2e<sup>-</sup>/2ATP. <sup>36,43–46</sup>

To clearly establish whether or not this claim is correct, the present work uses selected mediators as reducing agents that populate either FeP<sup>red</sup> or FeP<sup>sr</sup> as the respective dominant functioning state of the Fe protein under nitrogenase turnover conditions, as confirmed by electron paramagnetic resonance (EPR) spectroscopy. Advances in the ability to measure ATP hydrolysis with high fidelity, and to precisely measure electrons transferred by quantifying H<sub>2</sub> evolved establish the stoichiometric relationship of hydrolyzed ATP per electron transferred in each Fe protein cycle.

# **RESULTS AND DISCUSSION**

# The reduced states of Fe protein in the resting state and under turnover conditions under Ar

Dithionite (DT) is typically used to reduce FeP<sup>ox</sup> to FeP<sup>red</sup> having its associated cluster in the  $[4\text{Fe-}4\text{S}]^{1+}$  with a paramagnetic  $S = \frac{1}{2}$  spin state, which can be quantified by EPR spectroscopy (**Figure 2A**). <sup>16,18,19</sup> As previously assigned, use of MV<sup>++</sup> or Fld<sup>HQ</sup> as reductant generates the diamagnetic S = 0 all-ferrous state FeP<sup>sr</sup>, which therefore does not exhibit an EPR signal. <sup>34,36</sup> Other negative potential reductants, such as Eu(II)-L (L = EDTA, EGTA, or DTPA) or Ti(III)-citrate, can also reduce the Fe protein to the FeP<sup>sr</sup> state, but in these cases the  $[4\text{Fe-}4\text{S}]^0$  cluster is paramagnetic having S = 4

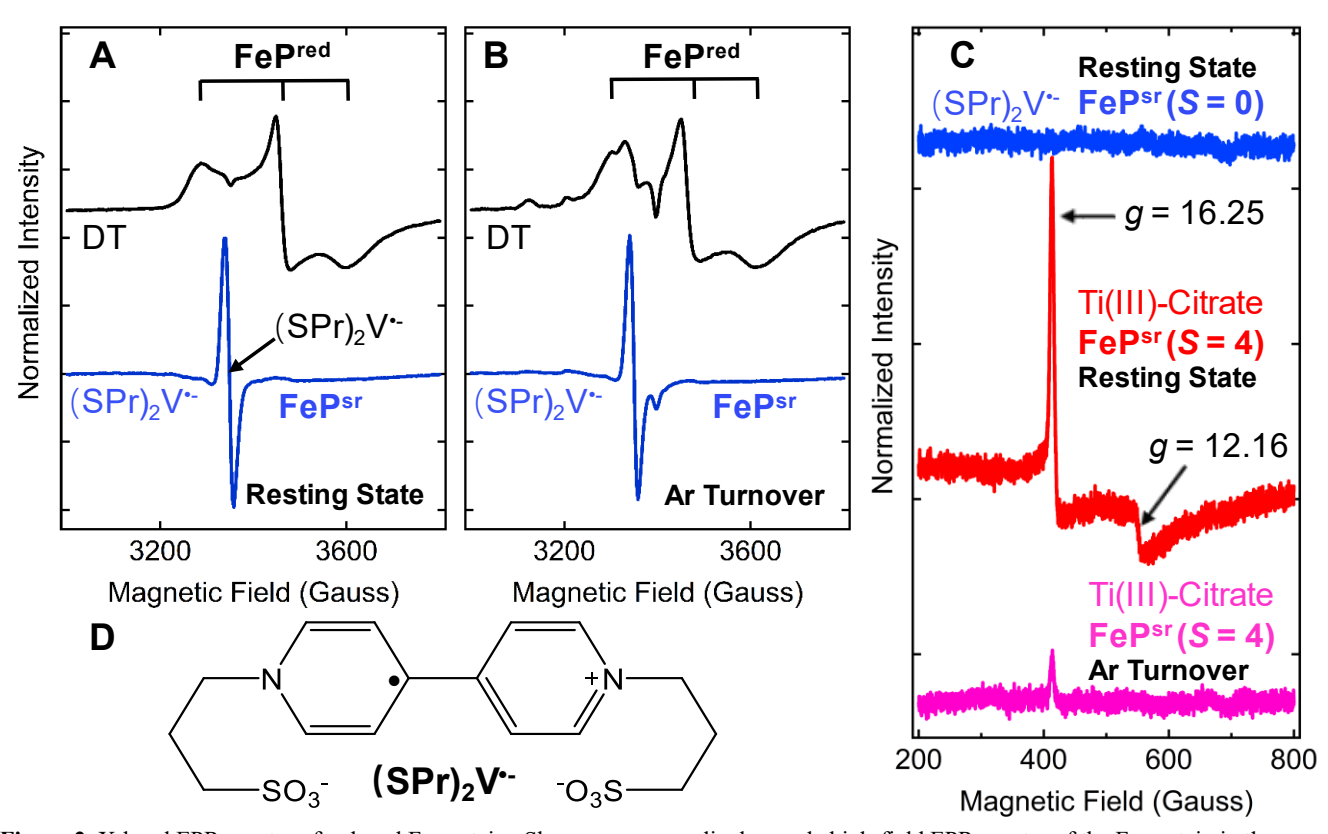


Figure 2. X-band EPR spectra of reduced Fe protein. Shown are perpendicular mode high-field EPR spectra of the Fe protein in the resting state (panel **A**) or under turnover with MoFe protein (panel **B**) with the reductant dithionite (DT, black traces) or (SPr)<sub>2</sub>V<sup>-</sup> (blue traces), and parallel mode low-field EPR spectra of the Fe protein (panel **C**) in the resting state with the reductant (SPr)<sub>2</sub>V<sup>-</sup> (blue trace) or Ti(III)-citrate (red trace) and under turnover with MoFe protein (magenta trace). Panel **D** shows the structure of (SPr)<sub>2</sub>V<sup>-</sup>. The EPR samples for perpendicular mode studies contained either 50 μM (panels **A** and **B**) or for parallel mode studies contained 110 μM Fe protein (panels **C**) in MOPS buffer (200 mM, pH 7.3) with 20 mM MgATP and an ATP-regenerating system (see Experimental Section) with either 20 mM DT or 2.5 mM (SPr)<sub>2</sub>V<sup>-</sup> (panels **A** and **B**), or 6.5 mM (SPr)<sub>2</sub>V<sup>-</sup> or 7.3 mM Ti(III)-citrate (panel **C**). The turnover samples also contained 5 μM MoFe protein resulting in [FeP]:[MoFeP] = 10:1 for perpendicular mode and [FeP]:[MoFeP] = 22:1 for parallel mode EPR studies, and were freeze-quenched after incubation for *ca*. 25 sec at room temperature. Perpendicular mode EPR conditions (panels **A** and **B**): temperature, 12 K; microwave frequency, 9.38 GHz; microwave power, 20 mW; modulation amplitude, 8.14 G; time constant 20.48 ms. Each trace is the sum of five scans. Parallel mode EPR conditions (panel **C**): temperature, 6.3 K; microwave frequency, 9.38 GHz; microwave power, 21 mW; modulation amplitude, 4 G; acquisition time, 35 min (blue trace), 24 min (red trace), and 50 min (magenta trace).

the super-reduced Fe protein has not been determined,  $^{19,39}$  but it is important to recognize that two different super-reduced states can exist and therefore need to be evaluated individually. Here, the one electron-reduced radical anion of a viologen derivative, 1,1'-bis(3-sulfonatopropyl)-4,4'-bipyridinium ((SPr)<sub>2</sub>V·,  $E_{\rm m}=$  -400 mV)<sup>47</sup> (**Figure 2D**) was used to reduce the Fe protein to the super-reduced [4Fe-4S]<sup>0</sup> state as confirmed by the absence of the S=1/2 [4Fe-4S]<sup>1+</sup> EPR signal (**Figure 2A and S1**). This mediator has been shown to be effective in supporting *in vitro* nitrogenase catalysis. The [4Fe-4S]<sup>0</sup> in this FePsr protein thus generated is diamagnetic (S=0), as supported here by the absence of the  $g\approx 16.4$  EPR signal associated with the S=4 state<sup>35,41</sup> that appears in the low-field region of the parallel mode EPR spectrum (**Figure 2C**). This assignment is consistent with that for the FePsr protein generated with the physiologic reductant Fld<sup>HQ</sup>. 36

When DT-reduced Fe protein is mixed with a reaction cocktail that includes MgATP, an ATP regenerating system, and MoFe protein, steady-state turnover is rapidly achieved and persists for at least 1

min when high protein concentrations suitable for EPR analysis are used. When the turnover is conducted under an atmosphere of argon, protons from solution are reduced to H2 as the sole catalytic product. Under such steady-state conditions, the solution can be rapidly frozen in liquid N2 to quench the reaction at a fixed time for analysis by low-temperature EPR.<sup>26</sup> When such assays are conducted using an excess of Fe protein over MoFe protein ([FeP]:[MoFeP] = 10:1), most of the Fe protein is unbound from the MoFe protein and predominantly exists as EPR-active FePred (Figure 2B). In contrast, when the same experiment is conducted using (SPr)<sub>2</sub>V\*- in place of DT, the quenched steady-state sample shows no Fe protein EPR signal, consistent with the unbound majority of the Fe protein being in the super-reduced, S = 0 state (Figures 2B and 2C). Hence, the Fered protein is the dominant functioning species during nitrogenase turnover with DT as reductant, while with  $(SPr)_2V^{\bullet}$  as reductant, it is the Fe<sup>sr</sup> (S=0) protein.

Analysis of the number of ATP hydrolyzed per electron transferred for nitrogenase catalysis

The analysis of H<sub>2</sub> formed during argon turnover provides a highly accurate way to quantify electron transfer because under these experimental conditions H<sub>2</sub> is the only catalytic product. To evaluate the ATP hydrolyzed per each electron transfer event, steady-state turnover assays under Ar were conducted, but in the absence of an ATP-regenerating system and over shorter times (1-2 min), to minimize the potential ADP inhibitory effect on nitrogenase catalysis, <sup>16</sup> after which the reaction was quenched with addition of 5 M NaCl aqueous solution.<sup>48</sup> All experimental turnover samples were accompanied by parallel control samples having the same component concentrations and reaction conditions except with addition of the quenching reagent prior to initiating nitrogenase catalysis. Using the corresponding turnover and control quenched samples, a highly sensitive Malachite green-based colorimetric assay (see Experimental Section and Figure S2) was used to measure the Pi and, hence, MgATP hydrolysis associated with the H2 formation. In this way, it was possible to establish the amount of ATP hydrolyzed for each electron transfer event occurring at fixed times during steadystate turnover.

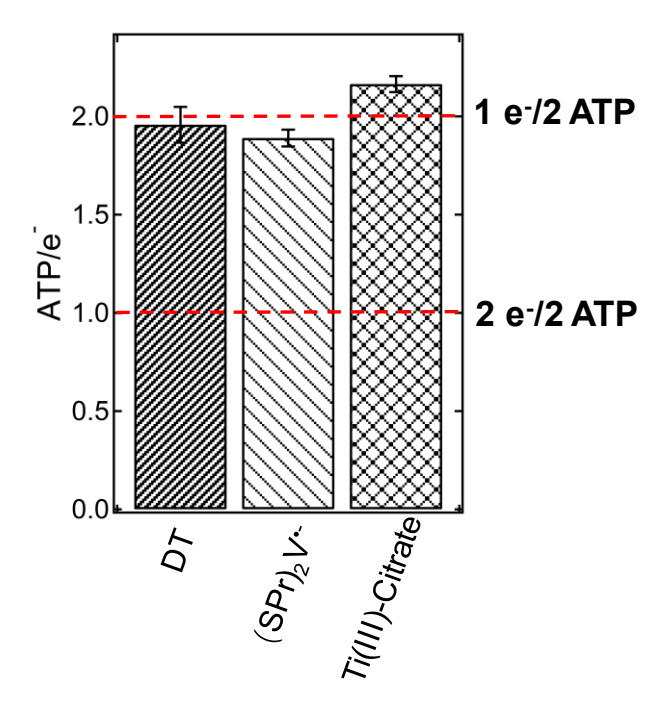


**Figure 3**. Ratio of ATP per electron (ATP/e<sup>-</sup>). Shown is the ratio of ATP hydrolyzed per electron accumulated in H<sub>2</sub> (ATP/e<sup>-</sup>) during a steady-state turnover under Ar with different reductants: DT, (SPr)<sub>2</sub>V<sup>-</sup>, or Ti(III)-citrate. All assays were conducted in a MOPS buffer (100 mM, pH 7.3) with *ca.* 10 mM MgATP in the absence of ATP-regenerating system with either 5 mM DT, 3.5 mM (SPr)<sub>2</sub>V<sup>-</sup>, or 7.3 mM Ti(III)-citrate as reductant. Following a 2-min pre-incubation at 30 °C, the reactions were initiated and incubated for 1 min before quenching. For DT and Ti(III)-citrate assays, a final concentration of 0.42 μM MoFeP and *ca.* 8 μM FeP was used. For (SPr)<sub>2</sub>V<sup>-</sup> assays, a final concentration of 0.5 μM MoFeP and *ca.* 4 μM FeP were used.

*DT as reductant:* As shown in Figure 3, when DT is used as reductant,  $1.96 \pm 0.09$  ATP are hydrolyzed for each electron transfer event with the Fe protein utilizing the [4Fe-4S]<sup>2+/1+</sup> couple. These findings are consistent with the findings from a number of earlier studies.<sup>2,7,16,32,44</sup>

 $(SPr)_2V^-$  as reductant: During Ar turnover when  $(SPr)_2V^-$  is used as reductant, and thus a high percentage of the Fe protein is in the EPR-silent, super-reduced (FePsr) state previously assigned as being diamagnetic (S=0), the corresponding analysis of electrons

consumed and ATP hydrolyzed, again indicates that ~2 ATP are hydrolyzed for each electron transfer event: ATP/e $^-$  of 1.89  $\pm$  0.04, **Figure 3**. This behavior with (SPr)<sub>2</sub>V $^-$  as the reductant persists upon altering the Fe protein to MoFe protein ratio (**Figure S3**), the reaction time (**Figure S4**), varying ATP concentration (**Figure S5**), or varying total MoFe protein concentration (**Figure S6**): in no case was a ratio lower than ~2ATP/e $^-$  observed. In short, the FePsr (S=0) protein is observed to deliver only one electron to MoFe protein with hydrolysis of two ATP per Fe protein cycle under the range of conditions examined here.

Ti(III)-citrate as reductant: Parallel studies were conducted using Ti(III)-citrate as reductant,<sup>49</sup> which was shown to produce the FePss protein in a S = 4 state.<sup>34</sup> Earlier studies suggested this Ti(III)citrate reduced FePsr state might transfer two electrons per Fe protein cycle coupled to the hydrolysis of two ATP (ATP/ $e^- = 1$ ). 43-46To examine the ATP/e ratio with this reductant, experiments were carried out using Ti(III)-citrate (Figure S7) (7.3 mM) and the same nitrogenase component protein concentrations used in the earlier work, 43,45 where results were interpreted to indicate that in aggregate only one ATP is consumed for each electron transfer. As shown in Figure 3, the present high-precision measurements clearly reveal there is no such change in behavior when Ti(III)citrate is used as the reductant: the ratio of ATP hydrolyzed per electron transferred is 2.16 ± 0.04, Moreover, this result was extended by varying the [FeP]: [MoFeP] molar ratios, with use of either 20:1 (Figure 3) or 5:1, and through variation of the Ti(III)citrate concentration (Figure S8).

The equivalent behavior of DT and Ti(III)-citrate as reductants is directly confirmed by noting that the total H<sub>2</sub> formed in a fixed amount of reaction time (specific activity) is essentially the same with either DT or Ti(III)-citrate as reductant (**Figure S9**), which is consistent with the observations in previous reports<sup>42,44</sup> with these two reductants for nitrogenase catalysis. The rate-limiting process in H<sub>2</sub> production is the Fe-protein cycle, and it is controlled not by the electron delivery to MoFe protein, but by release of Pi subsequent to ATP hydrolysis.<sup>6</sup> If FeP<sup>sr</sup> was delivering 2e<sup>-</sup> per Fe protein cycle (hydrolysis of two ATP), then the amount of H<sub>2</sub> formed per time would be twice that observed when the FeP<sup>red</sup> was operative (DT as reductant), delivering one-electron per Fe protein cycle.

To gain insight into the discrepancy between the ATP/e- values with Ti(III)-citrate as the reductant measured in this work and those previously reported, we determined that treatment of the Fe protein with an excess of Ti(III)-citrate does indeed form predominantly the FePsr, S = 4 state, through observation of its EPR signal at  $g \approx$ 16.3 in the parallel mode (Figure 2C).<sup>35,50</sup> In contrast, the EPR spectrum taken for the sample trapped during turnover in the presence of MoFe protein shows a greatly diminished g = 16.3 signal intensity, indicating the majority of the Fe protein is not in the S =4 state. A review of the literature explains this result. Earlier work suggested that although Ti(III)-citrate can reduce the Fe protein to the FePsr state, the kinetics of this reaction is slow. 42,43 The EPR observations during turnover reported here can thus be reasonably explained as Ti(III)-citrate reduction being unable to keep up with the electron transfer for substrate reduction. In short, in the steadystate, the Fe protein does not exist primarily as the FePsr state, as previously assumed, 42 but not measured. Instead, the EPR studies reported here suggest that it is the FePred ([4Fe-4S]1+) state that is the dominant when Ti(III)-citrate is the reductant under turnover conditions, with the FePsr ([4Fe-4S] $^{0}$ , S=4) state being a minor species (Figures 2C).

The diminished g = 16.3 signal for FePsr (S = 4) during turnover with Ti(III)-citrate as reductant implies that most of the Fe protein is in its one-electron reduced state, FePred ( $S = \frac{1}{2}$ ), which should be

observable in perpendicular-mode. Unfortunately, due to the presence of high concentration of EPR active Ti(III)-citrate ( $S = \frac{1}{2}$ ), the relatively low concentration of FePred ( $S = \frac{1}{2}$ ) signal was overwhelmed and could not be clearly seen in **Figure S1**.

To summarize the findings with Ti(III)-citrate as reductant, the results in the present work are not consistent with the earlier suggestion that the FeP<sup>sr</sup> state (S=4) transfers two electrons per Fe protein cycle coupled to the hydrolysis of two ATP, with FeP<sup>ox</sup>/FeP<sup>sr</sup> ([4Fe-4S]<sup>2+/0</sup>) as the operative redox couple when using Ti(III)-citrate.<sup>43–46</sup> The data presented here instead shows that under the conditions utilized here, Ti(III)-citrate reduced Fe protein delivers  $1 e^{-}$  per Fe protein cycle (2ATP/1e<sup>-</sup>) The SI presents a discussion of factors that could have led the earlier work astray.

**Eu(II)-L** as reductant: We tested another reductant that has been used with nitrogenase, Eu(II)-L, with different ligands (L) creating reductants with different (negative) potentials.  $^{40,41,51}$  There is no report to date addressing the compatibility of this reductant for nitrogenase catalysis in the presence of both nitrogenase component proteins and MgATP, although there are some reports that Eu(II)-L can support certain catalytic features of the individual Fe protein or MoFe protein.  $^{11,18,41,52}$  For example, several Eu(II)-L reductants have been shown to reduce Fe protein to FePsr (S=4).  $^{40,41}$  However, we find that Eu(II)-EDTA ( $E_{\rm m}=-840$  mV vs NHE) or Eu(II)-EGTA ( $E_{\rm m}=-880$  mV vs NHE)  $^{40,51-53}$  cannot drive nitrogenase catalysis above background H<sub>2</sub> formation when used in place of DT (**Figure S10 and S11**).

The result of adding sulfite to Eu(II)-EGTA reaction mixtures was further investigated, as suggested by a recent report. <sup>54</sup> It was found that when sulfite was added to Eu(II)-EGTA containing solutions before initiation of the reaction, the yellow color of Eu(II)-EGTA disappeared in less than one minute indicating the oxidation of Eu(II)-EGTA by sulfite. The resulting solution was able to drive nitrogenase catalysis at a level similar to an equivalent concentration of DT (**Figure S12**). These combined observations explain the reported effect of sulfite addition. They indicate that sulfite is reduced by Eu(II)-EGTA to SO<sub>2</sub>\*, the active redox species involved in nitrogenase reduction when dithionite is used as the artificial electron source. <sup>55</sup> These results show that it is inappropriate to draw mechanistic conclusions when the combination of Eu(II)-L and sulfite is used as a source of reducing equivalents during *in vitro* nitrogenase catalysis. <sup>54</sup>

Flavodoxin/DT as reductant: One of the physiological reductants for nitrogenase is the flavodoxin (Fld) protein and it has been shown that the  $Fld^{HQ}$  form can reduce Fe protein to the  $FeP^{sr}$  (S = 0) state. 24,25,56,57 Moreover, it has been used in in vitro studies suggesting 1ATP/e-. 36,43 However, it is hard to apply Fld<sup>HQ</sup> as the sole bulk reductant for in vitro steady-state kinetic measurements, 6,36,43 due to challenges in maintaining effective concentrations of the hydroquinone state, as well as an inhibitory effect on nitrogenase catalysis when Fld<sup>HQ</sup> is in high concentration. <sup>6</sup> Therefore, Fld is often used in combination with DT. 6,25,28,58 Recently, the application of this DT/Fld method in a steady-state kinetic study of nitrogenase revealed that the Pi release is the rate-limiting step in the Fe protein cycle with a determined ATP/ $e^- \approx 2.6$  However, the dominant redox state of Fe protein in that system was unknown. 18 Here, perpendicular-mode EPR now shows (Figure S13) that the  $S = \frac{1}{2}$  FePred ([4Fe-4S]<sup>1+</sup>) is the dominant functioning partner of MoFe protein when a combination of Fld and DT are used. The present measurements yield an ATP/e<sup>-</sup> of  $1.98 \pm 0.04$  (Figure S13) for this reducing system, in agreement with the previous report, but now explicitly showing the previously assumed involvement of FePred.

#### CONCLUSIONS

Results obtained in the present work demonstrate that during nitrogenase reduction of protons to form H<sub>2</sub>, both the FeP<sup>red</sup> ([4Fe-4S]<sup>1+</sup>) state and the all-ferrous FeP<sup>sr</sup> state transfer only one electron during each Fe protein cycle in a reaction that is linked to the hydrolysis of two ATP (**Figure 1C**). Thus, for proton reduction, a stoichiometry of 1 e<sup>-</sup> transfer coupled to hydrolysis of two ATP as a minimum for each Fe protein cycle is utilized. It should furthermore be emphasized that although an all-ferrous [4Fe-4S] cluster of the Fe protein can function for *in vitro* nitrogenase catalysis, there is no evidence to suggest which redox couple of the Fe protein dominates *in vivo* under different physiological conditions.

## **EXPERIMENTAL SECTION**

General procedures. All chemicals, unless otherwise noted, were obtained from Sigma-Aldrich (St. Louis, MO) and used without further purification. Adenosine-5'-triphosphate (ATP, disodium trihydrate, Ultra-Pure) was purchased from Gold Biotechnology (St. Louis, MO). Sodium citrate dihydrate and anhydrous sodium sulfite were purchased from Avantor Performance Materials (Center Valley, PA). Hydrogen and argon gases were purchased from Air Liquide America Specialty Gases LLC (Plumsteadville, PA). The argon gas was passed through an activated copper-catalyst to remove dioxygen contamination prior to use. A. vinelandii strains DJ995 (wild type MoFe protein) and DJ884 (wild type Fe protein) were grown, and nitrogenase proteins were expressed and purified as previously described.<sup>59</sup> Flavodoxin (Fld, NifF) was expressed and purified from E. coli as described before. 6,60 All proteins were greater than 95% pure as confirmed by SDS-PAGE analysis using Coomassie blue staining. The Fld contains about 56% FMN as the active site content determined with a procedure published before,<sup>6</sup> and was used as its semi-quinone form. 1,1'-bis(3-sulfonatopropyl)-4,4'-bipyridinium ((SPr)<sub>2</sub>V) was synthesized and a stock solution containing 250 mM (SPr)<sub>2</sub>V\* with 500 mM KCl was prepared by bulk electrolysis as described before.<sup>47</sup> The Malachite Green Phosphate Assay Kit (POMG-25H) was purchased from Bioassay Systems. Proteins and buffers were handled anaerobically in septum-sealed serum vials under an inert atmosphere (argon or dinitrogen), on a Schlenk vacuum line, or anaerobic glove box (Teledyne Analytical Instruments, MO-10-M, Hudson, NH). The transfer of gases and liquids were done with gastight syringes.

EPR. For resting state samples in X-band tubes, a final concentration of 50 µM Fe protein was added to a 200 mM MOPS buffer, pH 7.3, containing 20 mM ATP, 20 mM MgCl<sub>2</sub>, 30 mM phosphocreatine, ca. 0.4 mg/mL creatine phosphokinase, and 1 mg/mL bovine serum albumin, with either 20 mM sodium dithionite (DT), or 20 mM DT and 200 µM Fld, or 2.5 mM (SPr)<sub>2</sub>V<sup>--</sup> as reductant. For turnover samples, a final concentration of 5 µM MoFe protein was contained in the aforementioned buffer system before the addition of the Fe protein to start the reaction. After the addition of Fe protein, all samples were incubated at room temperature for ca. 20-25 sec. Then an aliquot of ca. 300 µL of reaction mixture was transferred into 4-mm calibrated quartz EPR tubes and rapidly frozen in a hexane/liquid nitrogen slurry and were stored in liquid nitrogen for EPR analysis. All Q-band EPR samples were prepared with 110 μM Fe protein and same methods with different reductants (Figure S1). The samples for parallel mode EPR studies were prepared in X-band tubes with the same component concentrations as those in Q-band samples.

Continuous-wave (CW) X-band EPR spectra were recorded using a Bruker ESP-300 spectrometer with an EMX PremiumX microwave bridge and an EMX<sup>PLUS</sup> standard resonator in perpendicular mode, equipped with an Oxford Instruments ESR900 continuous helium flow cryostat using VC40 flow controller for helium gas. Spectra were recorded at the following conditions: temperature, ~12 K or otherwise stated in the figure legends; microwave frequency, ~9.38 GHz; microwave power, 20 mW; modulation frequency, 100 kHz; modulation amplitude, 8.14 G; time constant, 20.48 ms. Each spectrum is the sum of five scans as indicated for each data set as in the figure legends. To evaluate the spin state of Fe protein reduced with 2.5 mM (SPr)<sub>2</sub>V<sup>\*</sup>, an increased microwave power (50mW) was applied in the low-field range (300-700 Gauss) to inspect any possible integer spin species (*S* = 4) with 5 scans at 12 K with other parameters unchanged.

Preparation of Ti(III)-citrate stock solution. Ti(III)-citrate solution was prepared by addition of 48  $\mu$ L Ti(III)Cl<sub>3</sub> solution (ca. 30% (2.60 M) Ti(III)Cl<sub>3</sub> in ca. 10% (3.66 M) HCl solution) to a pre-mixture of 500  $\mu$ L of 500 mM sodium citrate solution and 300  $\mu$ L of 1 M Tris base solution, giving a final concentration of Ti(III)-citrate is about 146 mM with a [Ti]:[citrate] =1:2. It should be noted that the 1 M Tris base solution was critical to neutralize the hydrochloric acid in Ti(III)Cl<sub>3</sub> and bring the final pH to an estimated range of 7-8. The spectrum of this Ti(III)-citrate solution was evaluated by UV-vis on a Cary 50 Bio UV-Visible spectrometer (**Figure S7**).

Preparation of Eu(II)-L stock solutions. The Eu(II)-L stock solution was prepared by dissolving an amount of Eu(II)Cl<sub>2</sub> with either a 250 mM EDTA (ethylenediaminetetraacetic acid disodium salt) or EGTA (ethylene glycol-bis( $\beta$ -aminoethyl ether)-N,N,N',N'-tetraacetic acid tetrasodium salt) solution at pH 8.0. For the data presented in **Figure S11**, the [Eu(II)]:[L] = 6:5. For those presented in **Figure S10** and **S12**, the [Eu(II)]:[L] = 1:1.

Determination of the ratio of hydrolyzed ATP per electron (ATP/e-) transferred for nitrogenase catalysis under Ar. To eliminate interference from the hydrolysis of phosphocreatine on quantification of inorganic phosphate (Pi), the reactions were carried out in 9.4 mL sealed serum vials with 1 mL of solution containing 100 mM MOPS reaction buffer, pH 7.3, containing only MgATP and corresponding reductants in the absence of an ATP regeneration system (phosphocreatine, creatine phosphokinase, and BSA) as specified in each figure legend. The concentrations of ATP and MgCl2 are equal in all cases. All reaction mixtures were pre-incubated in a water bath with shaking (160 rpm) at 30 °C for 2 min prior to starting the reaction by addition of a protein mixture of MoFe and Fe proteins. For the effect of component ratio studies with (SPr)<sub>2</sub>V<sup>-</sup> as reductant, the Fe protein was added to the reaction mixture containing MoFe protein to start the reactions. After the noted reaction time, the reactions were quenched by addition of 500 μL of 5M NaCl solution to the reaction mixture. To obtain proper backgrounds for H2 and Pi quantification for each set of experiments, the corresponding control experiments were done with same component ratios, and incubation time except that the quenching agent (NaCl) was added to the reaction mixture before initiation of the reactions. The total number of electrons transferred during turnover was determined based on the quantification of H2 formation after subtracting the backgrounds and adjusted to the proper atmospheric pressures in the laboratory (ca. 640 mmHg, Logan, Utah) as described before. 61 The amount of hydrolyzed ATP as formation of Pi was determined with a commercial assay kit (Malachite Green Phosphate Assay Kit, POMG-25H, BioAssay Systems) and a procedure slightly modified based the protocol provided by BioAssay

Systems. Typically, an aliquot of 10 or 20  $\mu$ L of the quenched reaction mixture was taken out of the reaction and diluted to 1 mL with 1.25 M NaCl solution with final ATP concentrations less than 0.2 mM. Then 200  $\mu$ L of assay reagent mixture of Reagent A and B in a ratio of 100:1 (v/v) was added to the diluted reaction mixture. The final mixture was incubated at room temperature for 30 min before recording the absorbance at 620 nm. A Pi standard curve was created with the 1 mM Pi standard solution provided by Bio-Assay Systems with the assay kit (**Figure S2**). The presented ATP/e<sup>-</sup> data were derived with the quantified Pi and H<sub>2</sub> after subtraction of proper backgrounds from appropriate control experiments as mentioned above.

## **ASSOCIATED CONTENT**

# **Supporting Information**

The Supporting Information is available free of charge on the ACS Publications website.

Detailed Materials and Methods, Experimental procedures, and supporting data and figures are included.

#### **Protein Accession IDs**

Nitrogenase molybdenum-iron protein alpha chain – NifD, Uni-ProtKB P07328

Nitrogenase molybdenum-iron protein beta chain - NifK, Uni-ProtKB P07329

Nitrogenase iron protein 1 – NifH, UniProtKB P00459

#### **AUTHOR INFORMATION**

# **Corresponding Authors**

Zhi-Yong Yang — Department of Chemistry and Biochemistry, Utah State University, Logan, Utah 84322, United States; orcid.org/0000-0001-8186-9450; Email: zhiyong.yang@usu.edu Lance C. Seefeldt — Department of Chemistry and Biochemistry, Utah State University, Logan, Utah 84322, United States; orcid.org/0000-0002-6457-9504; Email: lance.seefeldt@usu.edu

#### **Authors**

Artavazd Badalyan – Department of Chemistry and Biochemistry, Utah State University, Logan, Utah 84322, United States; orcid.org/0000-0002-6933-6181

Brian M. Hoffman – Department of Chemistry, Northwestern University, Evanston, Illinois 60208, United States; orcid.org/0000-0002-3100-0746

Dennis R. Dean – Department of Biochemistry, Virginia Polytechnic Institute and State University, Blacksburg, Virginia 24061, United States; orcid.org/0000-0001-8960-6196

#### Notes

The authors declare no competing financial interest.

#### **ACKNOWLEDGMENT**

We thank Ms. Maowei Hu and Dr. Tianbiao Liu at Utah State University for kindly providing the synthesized (SPr)<sub>2</sub>V. We thank Dr. Dmitriy Lukoyanov at Northwestern University for kind help on Qband EPR studies and Dr. Brian Bennett at Marquette University for parallel mode EPR examination. The parallel mode EPR study was supported by an NSF-MRI grant under award to BB (CHE-1532168). This work was supported by the U.S. Department of Energy, Office of Science, Basic Energy Sciences (BES) under awards to LCS (DE-SC0010687) and DRD (DE-SC00108343) and by the NSF under an award to BMH (MCB-1908587).

#### **REFERENCES**

- (1) Burris, R. H.; Roberts, G. P. Biological Nitrogen Fixation. *Annu. Rev. Nutr.* **1993**, *13*, 317–335. https://doi.org/10.1146/annurev.nu.13.070193.001533.
- (2) Ljones, T.; Burris, R. H. ATP Hydrolysis and Electron Transfer in the Nitrogenase Reaction with Different Combinations of the Iron Protein and the Molybdenum-Iron Protein. *Biochim. Biophys. Acta* **1972**, *275* (1), 93–101. https://doi.org/10.1016/0005-2728(72)90027-8.
- (3) Hageman, R. V.; Burris, R. H. Nitrogenase and Nitrogenase Reductase Associate and Dissociate with Each Catalytic Cycle. *Proc. Natl. Acad. Sci. U.S.A.* **1978**, 75 (6), 2699–2702. https://doi.org/10.1073/pnas.75.6.2699.
- (4) Mortenson, L. E. Ferredoxin and ATP, Requirements for Nitrogen Fixation in Cell-Free Extracts of *Clostridium Pasteurianum*. *Proc. Natl. Acad. Sci. U.S.A.* **1964**, *52* (2), 272–279. https://doi.org/10.2307/72434.
- (5) Bulen, W. A.; Burns, R. C.; LeComte, J. R. Nitrogen Fixation: Hydrosulfite as Electron Donor with Cell-Free Preparations of *Azotobacter Vinelandii* and *Rhodospirillum Rubrum. Proc. Natl. Acad. Sci. U.S.A.* **1965**, *53* (3), 532–539. https://doi.org/10.2307/72270.
- (6) Yang, Z.-Y.; Ledbetter, R.; Shaw, S.; Pence, N.; Tokmina-Lukaszewska, M.; Eilers, B.; Guo, Q.; Pokhrel, N.; Cash, V. L.; Dean, D. R.; Antony, E.; Bothner, B.; Peters, J. W.; Seefeldt, L. C. Evidence That the Pi Release Event Is the Rate-Limiting Step in the Nitrogenase Catalytic Cycle. *Biochemistry* **2016**, *55*, 3625–3635. https://doi.org/10.1021/acs.biochem.6b00421.
- (7) Bulen, W. A.; LeComte, J. R. The Nitrogenase System from Azotobacter: Two-Enzyme Requirement for N<sub>2</sub> Reduction, ATP-Dependent H<sub>2</sub> Evolution, and ATP Hydrolysis. *Proc. Natl. Acad. Sci. U.S.A.* **1966**, *56* (3), 979–986. https://doi.org/10.2307/57683.
- (8) Eady, R. R. Structure–Function Relationships of Alternative Nitrogenases. *Chem. Rev.* **1996**, *96* (7), 3013–3030. https://doi.org/10.1021/cr950057h.
- (9) Eady, R. R. Current Status of Structure Function Relationships of Vanadium Nitrogenase. *Coord. Chem. Rev.* **2003**, *237* (1–2), 23–30. https://doi.org/10.1016/S0010-8545(02)00248-5.
- (10) Yang, Z.-Y.; Jimenez-Vicente, E.; Kallas, H.; Lukoyanov, D. A.; Yang, H.; Campo, J. S. M. del; Dean, D. R.; Hoffman, B. M.; Seefeldt, L. C. The Electronic Structure of FeV-Cofactor in Vanadium-Dependent Nitrogenase. *Chem. Sci.* **2021**, *12* (20), 6913–6922. https://doi.org/10.1039/D0SC06561G.
- (11) Jasniewski, A. J.; Lee, C. C.; Ribbe, M. W.; Hu, Y. Reactivity, Mechanism, and Assembly of the Alternative Nitrogenases. *Chem. Rev.* **2020**, *120* (12), 5107–5157. https://doi.org/10.1021/acs.chemrev.9b00704.
- (12) Schneider, K.; Müller, A. Iron-Only Nitrogenase: Exceptional Catalytic, Structural and Spectroscopic Features. In *Catalysts for Nitrogen Fixation*; Nitrogen Fixation: Origins, Applications, and Research Progress; Springer, Dordrecht, 2004; pp 281–307. https://doi.org/10.1007/978-1-4020-3611-8 11.
- (13) Hales, B. J. Alternative Nitrogenase. *Adv. Inorg. Biochem.* **1990**, *8*, 165–198.
- (14) Seefeldt, L. C.; Yang, Z.-Y.; Lukoyanov, D. A.; Harris, D. F.; Dean, D. R.; Raugei, S.; Hoffman, B. M. Reduction of Substrates by Nitrogenases. *Chem. Rev.* **2020**, *120* (12), 5082–5106. https://doi.org/10.1021/acs.chemrev.9b00556.
- (15) Harris, D. F.; Lukoyanov, D. A.; Kallas, H.; Trncik, C.; Yang, Z.-Y.; Compton, P.; Kelleher, N.; Einsle, O.; Dean, D. R.; Hoffman, B. M.; Seefeldt, L. C. Mo-, V-, and Fe-Nitrogenases Use a Universal Eight-Electron Reductive-Elimination Mechanism to Achieve N<sub>2</sub> Reduction. *Biochemistry* **2019**, *58* (30), 3293–3301. https://doi.org/10.1021/acs.biochem.9b00468.
- (16) Burgess, B. K.; Lowe, D. J. Mechanism of Molybdenum Nitrogenase. *Chem. Rev.* **1996**, *96*, 2983–3012. https://doi.org/10.1021/cr950055x.
- (17) Hoffman, B. M.; Lukoyanov, D.; Yang, Z.-Y.; Dean, D. R.; Seefeldt, L. C. Mechanism of Nitrogen Fixation by Nitrogenase: The next Stage. *Chem. Rev.* **2014**, *114*, 4041–4062. https://doi.org/10.1021/cr400641x.
- (18) Rutledge, H. L.; Tezcan, F. A. Electron Transfer in Nitrogenase. *Chem. Rev.* **2020**, *120* (12), 5158–5193. https://doi.org/10.1021/acs.chemrev.9b00663.
- (19) Van Stappen, C.; Decamps, L.; Cutsail, G. E.; Bjornsson, R.; Henthorn, J. T.; Birrell, J. A.; DeBeer, S. The Spectroscopy of Nitrogenases. *Chem. Rev.* **2020**, *120* (12), 5005–5081. https://doi.org/10.1021/acs.chemrev.9b00650.

- (20) Einsle, O.; Rees, D. C. Structural Enzymology of Nitrogenase Enzymes. *Chem. Rev.* **2020**, *120* (12), 4969–5004. https://doi.org/10.1021/acs.chemrev.0c00067.
- (21) Thorneley, R. N. F.; Lowe, D. J. Kinetics and Mechanism of the Nitrogenase Enzyme. In *Molybdenum Enzymes*; Spiro, T. G., Ed.; Metal Ions in Biology; Wiley-Interscience Publications: New York, 1985; Vol. 7, pp 221–284.
- (22) Lowe, D. J.; Ashby, G. A.; Brune, M.; Knights, H.; Webb, M. R.; Thorneley, R. N. F. ATP Hydrolysis and Energy Transduction by Nitrogenase. In *Nitrogen Fixation: Fundamentals and Applications*; Tikhonovich, I. A., Provorov, N. A., Romanov, V. I., Newton, W. E., Eds.; Summerfield, R. J., Series Ed.; Springer Netherlands: Dordrecht, 1995; Vol. 27, pp 103–108. https://doi.org/10.1007/978-94-011-0379-4 14.
- (23) Seefeldt, L. C.; Hoffman, B. M.; Peters, J. W.; Raugei, S.; Beratan, D. N.; Antony, E.; Dean, D. R. Energy Transduction in Nitrogenase. *Acc. Chem. Res.* **2018**, *51*, 2179–2186.
- (24) Martin, A. E.; Burgess, B. K.; Iismaa, S. E.; Smartt, C. T.; Jacobson, M. R.; Dean, D. R. Construction and Characterization of an *Azotobacter Vinelandii* Strain with Mutations in the Genes Encoding Flavodoxin and Ferredoxin I. *J. Bacteriol.* **1989**, *171* (6), 3162–3167. https://doi.org/10.1128/jb.171.6.3162-3167.1989.
- (25) Yates, M. G. Electron Transport to Nitrogenase in Azotobacter Chroococcum: Azotobacter Flavodoxin Hydroquinone as an Electron Donor. *FEBS Letters* **1972**, *27* (1), 63–67. https://doi.org/10.1016/0014-5793(72)80410-1.
- (26) Seefeldt, L. C.; Hoffman, B. M.; Dean, D. R. Mechanism of Mo-Dependent Nitrogenase. *Annu. Rev. Biochem.* **2009**, *78* (1), 701–722. https://doi.org/10.1146/annurev.biochem.78.070907.103812.
- (27) Seefeldt, L. C.; Yang, Z.-Y.; Duval, S.; Dean, D. R. Nitrogenase Reduction of Carbon-Containing Compounds. *Biochim. Biophys. Acta* **2013**, *1827* (8), 1102–1111. https://doi.org/10.1016/j.bbabio.2013.04.003.
- (28) Simpson, F. B.; Burris, R. H. A Nitrogen Pressure of 50 Atmospheres Does Not Prevent Evolution of Hydrogen by Nitrogenase. *Science* **1984**, *224* (4653), 1095–1097. https://doi.org/10.1126/science.6585956.
- (29) Hoffman, B. M.; Lukoyanov, D.; Dean, D. R.; Seefeldt, L. C. Nitrogenase: A Draft Mechanism. *Acc. Chem. Res.* **2013**, *46* (2), 587–595. https://doi.org/10.1021/ar300267m.
- (30) Burns, R. C.; Bulen, W. A. ATP-Dependent Hydrogen Evolution by Cell-Free Preparations of *Azotobacter Vinelandii*. *Biochim. Biophys. Acta* **1965**, *105* (3), 437–445. https://doi.org/10.1016/S0926-6593(65)80229-6.
- (31) Winter, H. C.; Burris, R. H. Nitrogenase. *Annu. Rev. Biochem.* **1976**, 45 (1), 409–426. https://doi.org/10.1146/annurev.bi.45.070176.002205.
- (32) Watt, G. D.; Bulen, W. A.; Burns, A.; Hadfield, K. L. M. Stoichiometry, ATP/2e Values, and Energy Requirements for Reactions Catalyzed by Nitrogenase from *Azotobacter Vinelandii*. *Biochemistry*. **1975**, *14* (19), 4266–4272. https://doi.org/10.1021/bi00690a019.
- (33) Seefeldt, L. C.; Peters, J. W.; Beratan, D. N.; Bothner, B.; Minteer, S. D.; Raugei, S.; Hoffman, B. M. Control of Electron Transfer in Nitrogenase. *Curr. Opin. Chem. Biol.* **2018**, *47*, 54–59. https://doi.org/10.1016/j.cbpa.2018.08.011.
- (34) Watt, G. D.; Reddy, K. R. N. Formation of an All Ferrous Fe<sub>4</sub>S<sub>4</sub> Cluster in the Iron Protein Component of *Azotobacter Vinelandii* Nitrogenase. *J. Inorg. Biochem.* **1994**, *53* (4), 281–294. https://doi.org/10.1016/0162-0134(94)85115-8.
- (35) Angove, H. C.; Yoo, S. J.; Burgess, B. K.; Münck, E. Mössbauer and EPR Evidence for an All-Ferrous  $Fe_4S_4$  Cluster with S=4 in the Fe Protein of Nitrogenase. *J. Am. Chem. Soc.* **1997**, *119* (37), 8730–8731. https://doi.org/10.1021/ja9712837.
- (36) Lowery, T. J.; Wilson, P. E.; Zhang, B.; Bunker, J.; Harrison, R. G.; Nyborg, A. C.; Thiriot, D.; Watt, G. D. Flavodoxin Hydroquinone Reduces *Azotobacter Vinelandii* Fe Protein to the All-Ferrous Redox State with a *S* = 0 Spin State. *Proc. Natl. Acad. Sci. U.S.A.* **2006**, *103* (46), 17131–17136. https://doi.org/10.1073/pnas.0603223103.
- (37) Yao, W.; Gurubasavaraj, P. M.; Holland, P. L. All-Ferrous Iron–Sulfur Clusters. In *Molecular Design in Inorganic Biochemistry*; Rabinovich, D., Ed.; Structure and Bonding; Springer: Berlin, Heidelberg, 2014; pp 1–37. https://doi.org/10.1007/430 2012 81.
- (38) Guo, M.; Sulc, F.; Ribbe, M. W.; Farmer, P. J.; Burgess, B. K. Direct Assessment of the Reduction Potential of the [4Fe-4S]<sup>1+0</sup> Couple of the Fe Protein from *Azotobacter Vinelandii*. *J. Am. Chem. Soc.* **2002**, *124* (41), 12100–12101. https://doi.org/10.1021/ja026478f.

- (39) Tan, M.-L.; Perrin, B. S.; Niu, S.; Huang, Q.; Ichiye, T. Protein Dynamics and the All-Ferrous [Fe4S4] Cluster in the Nitrogenase Iron Protein. *Protein Sci.* **2016**, *25* (1), 12–18. https://doi.org/10.1002/pro.2772.
- (40) Vincent, K. A.; Tilley, G. J.; Quammie, N. C.; Streeter, I.; Burgess, B. K.; Cheesman, M. R.; Armstrong, F. A. Instantaneous, Stoichiometric Generation of Powerfully Reducing States of Protein Active Sites Using Eu(II) and Polyaminocarboxylate Ligands. *Chem. Commun.* **2003**, No. 20, 2590–2591. https://doi.org/10.1039/B308188E.
- (41) Solomon, J. B.; Rasekh, M. F.; Hiller, C. J.; Lee, C. C.; Tanifuji, K.; Ribbe, M. W.; Hu, Y. Probing the All-Ferrous States of Methanogen Nitrogenase Iron Proteins. *JACS Au* **2021**, *I* (2), 119–123. https://doi.org/10.1021/jacsau.0c00072.
- (42) Angove, H. C.; Yoo, S. J.; Münck, E.; Burgess, B. K. An All-Ferrous State of the Fe Protein of Nitrogenase: Interaction with Nucleotides and Electron Transfer to the MoFe Protein. *J. Biol. Chem.* **1998**, *273* (41), 26330–26337. https://doi.org/10.1074/jbc.273.41.26330.
- (43) Erickson, J. A.; Nyborg, A. C.; Johnson, J. L.; Truscott, S. M.; Gunn, A.; Nordmeyer, F. R.; Watt, G. D. Enhanced Efficiency of ATP Hydrolysis during Nitrogenase Catalysis Utilizing Reductants That Form the All-Ferrous Redox State of the Fe Protein. *Biochemistry.* **1999**, *38* (43), 14279–14285. https://doi.org/10.1021/bi991389+.
- (44) Jacobs, D.; Watt, G. D. Nucleotide-Assisted [Fe<sub>4</sub>S<sub>4</sub>] Redox State Interconversions of the *Azotobacter Vinelandii* Fe Protein and Their Relevance to Nitrogenase Catalysis. *Biochemistry.* **2013**, *52* (28), 4791–4799. https://doi.org/10.1021/bi301547b.
- (45) Nyborg, A. C.; Erickson, J. A.; Johnson, J. L.; Gunn, A.; Truscott, S. M.; Watt, G. D. Reactions of *Azotobacter Vinelandii* Nitrogenase Using Ti(III) as Reductant. *J. Inorg. Biochem.* **2000**, 78 (4), 371–381. https://doi.org/10.1016/S0162-0134(00)00066-0.
- (46) Nyborg, A. C.; Johnson, J. L.; Gunn, A.; Watt, G. D. Evidence for a Two-Electron Transfer Using the All-Ferrous Fe Protein during Nitrogenase Catalysis. *J. Biol. Chem.* **2000**, *275* (50), 39307–39312. https://doi.org/10.1074/jbc.M007069200.
- (47) Badalyan, A.; Yang, Z.-Y.; Hu, B.; Luo, J.; Hu, M.; Liu, T. L.; Seefeldt, L. C. An Efficient Viologen-Based Electron Donor to Nitrogenase. *Biochemistry* **2019**, *58*, 4590–4595. https://doi.org/10.1021/acs.biochem.9b00844
- (48) Katz, F. E. H.; Shi, X.; Owens, C. P.; Joseph, S.; Tezcan, F. A. Determination of Nucleoside Triphosphatase Activities from Measurement of True Inorganic Phosphate in the Presence of Labile Phosphate Compounds. *Anal. Biochem.* **2017**, 520, 62–67. https://doi.org/10.1016/j.ab.2016.12.012.
- (49) Seefeldt, L. C.; Ensign, S. A. A Continuous, Spectrophotometric Activity Assay for Nitrogenase Using the Reductant Titanium(III) Citrate. *Analytical Biochemistry* **1994**, *221* (2), 379–386. https://doi.org/10.1006/abio.1994.1429.
- (50) Yoo, S. J.; Angove, H. C.; Burgess, B. K.; Hendrich, M. P.; Münck, E. Mössbauer and Integer-Spin EPR Studies and Spin-Coupling Analysis of the [4Fe-4S]<sup>0</sup> Cluster of the Fe Protein from *Azotobacter Vinelandii* Nitrogenase. *J. Am. Chem. Soc.* **1999**, *121* (11), 2534–2545. https://doi.org/10.1021/ja9837405.

- (51) Botta, M.; Ravera, M.; Barge, A.; Bottaro, M.; Osella, D. Relationship between Ligand Structure and Electrochemical and Relaxometric Properties of Acyclic Poly(Aminocarboxylate) Complexes of Eu(II). *Dalton Trans.* **2003**, No. 8, 1628–1633. https://doi.org/10.1039/B211533F.
- (52) Danyal, K.; Rasmussen, A. J.; Keable, S. M.; Inglet, B. S.; Shaw, S.; Zadvornyy, O. A.; Duval, S.; Dean, D. R.; Raugei, S.; Peters, J. W.; Seefeldt, L. C. Fe Protein-Independent Substrate Reduction by Nitrogenase MoFe Protein Variants. *Biochemistry* **2015**, *54* (15), 2456–2462. https://doi.org/10.1021/acs.biochem.5b00140.
- (53) Paengnakorn, P.; Ash, P. A.; Shaw, S.; Danyal, K.; Chen, T.; Dean, D. R.; Seefeldt, L. C.; Vincent, K. A. Infrared Spectroscopy of the Nitrogenase MoFe Protein under Electrochemical Control: Potential-Triggered CO Binding. *Chem. Sci.* **2017**, 8, 1500–1505. https://doi.org/10.1039/C6SC02860H.
- (54) Lee, C. C.; Kang, W.; Jasniewski, A. J.; Stiebritz, M. T.; Tanifuji, K.; Ribbe, M. W.; Hu, Y. Evidence of Substrate Binding and Product Release via Belt-Sulfur Mobilization of the Nitrogenase Cofactor. *Nat. Catal.* **2022**, *5* (5), 443–454. https://doi.org/10.1038/s41929-022-00782-7.
- (55) Mayhew, S. G. The Redox Potential of Dithionite and  $SO_2^-$  from Equilibrium Reactions with Flavodoxins, Methyl Viologen and Hydrogen plus Hydrogenase. *Eur. J. Biochem.* **1978**, *85*, 535–547. https://doi.org/10.1111/j.1432-1033.1978.tb12269.x.
- (56) Klugkist, J.; Voorberg, J.; Haaker, H.; Veeger, C. Characterization of Three Different Flavodoxins from *Azotobacter Vinelandii. Eur. J. Biochem.* **1986**, *155* (1), 33–40. https://doi.org/10.1111/j.1432-1033.1986.tb09455.x.
- (57) Thorneley, R. N.; Deistung, J. Electron-Transfer Studies Involving Flavodoxin and a Natural Redox Partner, the Iron Protein of Nitrogenase: Conformational Constraints on Protein-Protein Interactions and the Kinetics of Electron Transfer within the Protein Complex. *Biochem. J.* **1988**, *253*, 587–595. https://doi.org/10.1042/bj2530587.
- (58) Hageman, R. V.; Burris, R. H. Kinetic Studies on Electron Transfer and Interaction between Nitrogenase Components from *Azotobacter Vinelandii*. *Biochemistry* **1978**, *17* (20), 4117–4124. https://doi.org/10.1021/bi00613a002.
- (59) Christiansen, J.; Goodwin, P. J.; Lanzilotta, W. N.; Seefeldt, L. C.; Dean, D. R. Catalytic and Biophysical Properties of a Nitrogenase Apo-MoFe Protein Produced by an *NifB*-Deletion Mutant of *Azotobacter Vinelandii*. *Biochemistry* **1998**, *37*, 12611–12623.
- (60) Bennett, L. T.; Jacobson, M. R.; Dean, D. R. Isolation, Sequencing, and Mutagenesis of the NifF Gene Encoding Flavodoxin from Azotobacter Vinelandii. *J. Biol. Chem.* **1988**, *263* (3), 1364–1369.
- (61) Lukoyanov, D.; Yang, Z.-Y.; Khadka, N.; Dean, D. R.; Seefeldt, L. C.; Hoffman, B. M. Identification of a Key Catalytic Intermediate Demonstrates That Nitrogenase Is Activated by the Reversible Exchange of N<sub>2</sub> for H<sub>2</sub>. *J. Am. Chem. Soc.* **2015**, *137*, 3610–3615.

